RSC Advances

ROYAL SOCIETY
OF CHEMISTRY

www.rsc.org/advances

Cuprous oxide (Cu_2O) nanocubes and microspheres are successfully fabricated by reducing of $CuCl_2$ upon addition of ascorbic acid as a reductive agent with assistance of carbon dots (C-dots).
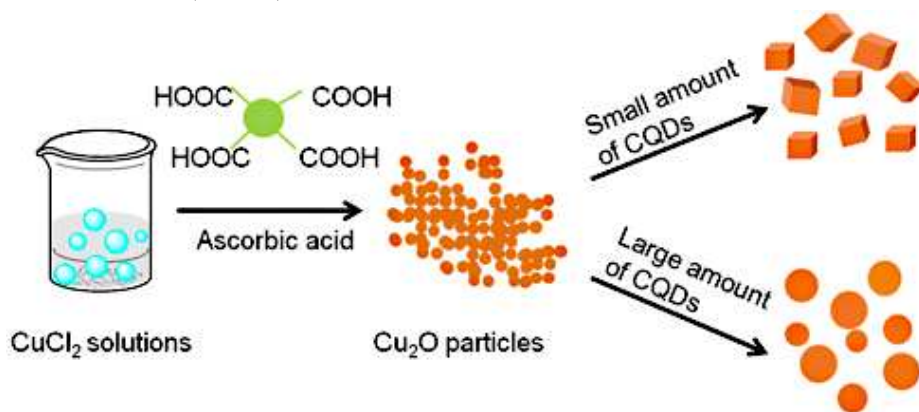
ARTICLE TYPE

Controllable synthesis of two different morphologies of Cu₂O particles with assistance of carbon dots

Xiaoyun Fan,*[a] Ning Hua[a,b], Jian Xu[b], Zhen Wang[a], Hanzhong Jia[a], Chuanyi Wang*[a]

Cuprous oxide (Cu₂O) nanocubes and microspheres are successfully fabricated by reducing of CuCl₂ upon addition of ascorbic acid as a reductive agent with assistance of carbon dots (C-dots). The average edge length of the cubes varies from 300 to 400 nm, while the spheres fall in the range of 0.7-2 μm. The possible mechanism has been explored. By HNO₃ treatment, various carbonyl functionalities are
10 introduced to the surfaces of C-dots, thus giving rise to dramatic effects on the morphologic changes of resultant Cu₂O crystals.

1.Introduction

Cuprous oxide (Cu₂O), an important p-type semiconductor with a direct band gap of about 2.2 eV, is a promising material
15 with applications in low-cost photo-voltaics [1] and high-efficiency photocatalysis [2], decomposition of water into O₂ and H₂ under visible light [3]. It is known that surface morphology is an important factor in determining the structural, physical, and chemical properties of nanoparticles [4-6]. In the past decade, much
20 effort has been devoted to shape-controlled synthesis of Cu₂O micro- and nanocrystals, such as liquid-phase synthesis of Cu₂O nanowires [7], nano-cubes [8], polyhedra [9], nanocage [10], and hollow spheres [11]. In these methods, the preferential adsorption of organic (ligands, polymers, surfactants) or inorganic (ions, gases)
25 agents, such as polyvinyl-pyrrolidone(PVP) [12], sodium dodecyl sulfate (SDS) [13], poly ethylene glycol (PEG) [14] and cetyltrimethylammonium bromide (CTAB) [15], ionic liquids [16] were generally required to control the morphologies and structures of the products. However, it remains a great challenge
30 to develop a green method for the synthesis of Cu₂O structures with micro-cubes and nanospherical morphologies.

Carbon quantum dots (CQDs) are the carbon nanoparticles that are luminescent and water soluble by surface oxidization or passivation and are non-toxic compared to semiconductor QDs [17].
35 The CQDs are generally small oxygenous carbon nanoparticles (<10 nm), and could be classified as the new zero-dimensional member in versatile carbon nanomaterials family. Typically displaying size and excitation wavelength dependent photoluminescence (PL) behavior, C-dots are attracting
40 considerable attention as nascent quantum dots, particularly for applications in which the size, cost, and biocompatibility of the label are critical [18]. C-dots contain many carboxylic acid moieties at their surface, thus imparting them with excellent water solubility and the suitability for subsequent functionalization with
45 various organic, polymeric, inorganic, or biological species.

Here, we report a synthesis of two different morphologies of Cu₂O particles with assistance of surface functionalized carbon dots. The cubic Cu₂O particles prepared this way are homogeneous in both shape and size. The average edge length of
50 the cubes varies from 300 to 400 nm, while the spheres are in the range of 700 nm-2 μm. The surface carbonyl acid unit is believed to play a key role in the morphology control.

2. Experiment

Analytical grade precursor salt (CuCl₂), ascorbic acid (C₆H₈O₆),
55 carbon quantum dots solutions, and NaOH were used as received without further purification. The crystal structures of Cu₂O powders were determined by X-ray diffraction (XRD) patterns using an Bruker D8 Advance with a Cu-Kα (λ=1.5418 Å) radiation and a nickel filter at room temperature in the angular
60 range from 10 to 80° (2θ) with a scanning step width of 0.02° and a fixed counting time of 1 s/step. The morphologies of the samples were observed on a scanning electron microscope (SEM) using a ZEISS SUPRA55VP apparatus. The absorption spectra of C-dots were measured by UV-Vis spectroscopy (Shimadzu Uv-
65 1800). Fluorescence spectra of carbon dots were measured on a Hitachi fluorescence spectrophotometer F-7000.

2.1 Fluorescent carbon nanoparticles were synthesized as follows

2 g glucose was dissolved in 30 mL 2% acetic acid solutions,
70 and then the mixture was sealed into a Teflon equipped stainless steel autoclave, which was then placed in a muffle furnace followed by hydrothermal treatment at 180 °C for 6 h. After the reaction, the autoclave was cooled down naturally. The obtained dark brown solution was centrifuged at a high speed (1w rpm) for
75 15 min to remove the less-fluorescent deposit. The brownish yellow supernatant after centrifugation was neutralized by Na₂CO₃, and then dialyzed against water through a dialysis membrane (MW cutoff 1000) for 1 day.

2.2 Surface passivation process of C-dots

Typically, 0.5 g of diamine-terminated oligomeric poly (ethylene glycol) $H_2NCH_2(CH_2CH_2O)nCH_2CH_2CH_2NH_2$ (nav=35, PEG1500N) was added to the C-dots solution and the mixture was heated to 120 °C for 12 h for surface passivation. Then the optically transparent and photoluminescent C-Dots solution was again purified via dialysis for 1 day. Finally, a clear, light yellow aqueous solution containing surface passivated C-dots was obtained.

2.3 Synthesis of Cu_2O particles

In a typical synthesis, $CuCl_2 \cdot 2H_2O$ (0.171 g) was dissolved into aqueous solution (100 mL). Then NaOH aqueous solution (10.0 mL, 2.0 M) was added dropwise into the above transparent light green solution. After stirring for 0.5 h, carbon quantum dots aqueous solution (0.05-0.1 M) and ascorbic acid solution (10.0 mL, 0.2 M) was added dropwise into the above solution. The mixture was reflected in the water-bath for 2 h at 80 °C. A turbid red liquid gradually formed. All of the procedures were carried out under constant stirring and heated at 80 °C. The resulting precipitate was separated from the solution by centrifugation at 10000 rpm for 5 min and washed several times with deionized water and ethanol. Then the sample was dried under vacuum at ambient temperature.

3. Results and Discussion

Transmission electron microscopy (TEM) C-dots reveals the formation of nearly spherical nanoparticles with average sizes in the range 4-9 nm (Figure 1).
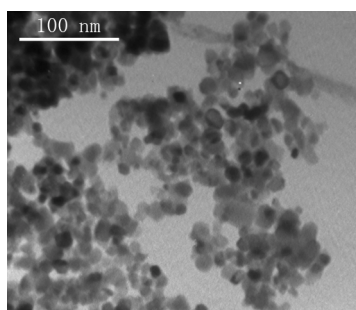

Figure 1.TEM images of C-dots

The UV-vis absorption spectrum of the C-dots has been recorded in Fig. S1 in supplementary information. The absorption spectrum in water reveals no distinct peaks in the Uv-vis region and absorption spectrum blue-shifts as the centrifuged speed increased, it is informed that the particles size become much smaller. The luminescent properties of the as-prepared C-dots have been explored see Fig. S2. As the excitation wavelength increases, the PL emissions red-shift accompanied continuously with an obvious decrease of PL intensity. An emission maximum appears at 443 nm when excited at 358 nm. It is also interesting to note that these photoluminescence properties are very similar to those observed with carbon nanoparticles obtained from candle soot [19]. FT-IR spectrum of the carbon dots is shown in Fig. S3, where an apparent absorption peak of -OH group at about 3400 cm^{-1} and an absorption peak of C=O group conjugated with condensed aromatic carbons at 1662 cm^{-1} appear, respectively. These data reveal that the obtained C-dots are rich in carboxylic groups. In addition, a negative zeta potential of nanoparticles was recorded (-3.25 mV) in aqueous solution, corroborating the presence of residual carboxylic groups at their surface.

Fig. 2 shows the X-ray diffraction of the prepared Cu_2O particles. High crystallinity is confirmed by the strong diffraction peaks, which match well with the standard pattern of cuprite (JCPDS No. 5-0667). Moreover, the other diffraction peaks belonging to possible impurities such as Cu and CuO could be detected.
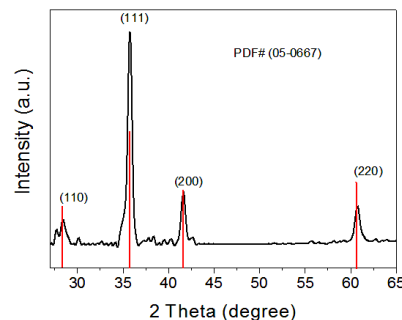

Figure 2. Powder X-ray diffraction pattern of the synthesized Cu_2O.The peaks are labeled with the standard cuprite reflections.

The SEM images of the Cu_2O samples are shown in Fig. 3a-3d. Cu_2O crystals with cubic and spherical shapes were obtained. Notably, these Cu_2O cubes are of unequal diameters from 300 to 400 nm. The average size of the spheres falls in the range 0.7- 2 μm.
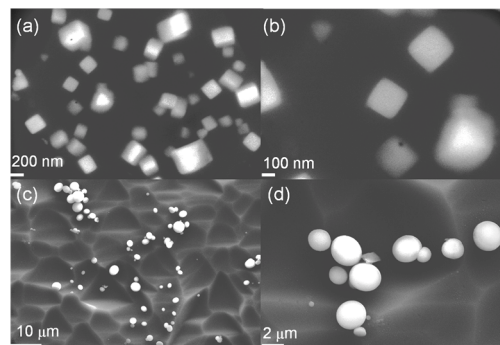

Figure 3. SEM images of the Cu_2O particles, (a) and (b) 0.05 M CQDs, (c) and (d) 0.1 M CQDs.

The corresponding energy-dispersive X-ray (EDX) analysis results are shown in Fig. 4. Cu and O are detected in the EDX, analysis and the elemental ratio of Cu:O is close to 2:1, further confirming that the obtained products are Cu_2O crystals. Note that Si peaks in images are attributed to the SEM platform used to support the specimen.
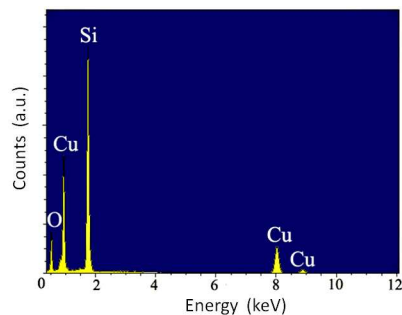
Figure 4. EDX and of Cu$_2$O particles. The Si signals of the EDX plots belong to the nickel grid used for particles deposition accompanying EDX analysis.

The morphology of Cu$_2$O synthesized without carbon dots is shown in Fig. S4. Without C-dots, the mixture of irregular Cu$_2$O agglomeration was formed. It can conclude that C-dots facilitate to stabilize Cu$_2$O particles with regular polyhedral shapes in aqueous solution and prevent their aggregation. The possible mechanism for the change of morphology of Cu$_2$O grown with and without carbon dots may be explained by the different bonding interactions between the carboxylic groups and the transition metals, and the carbon quantum dots behaves as the capping agent. As it has been known that the two oxygen atoms of the carboxylic group would bind to the Cu$_2$O, and carboxylic binds asymmetrically with the tilting angle close to zero [20]. The interaction between carboxylic group and Cu$_2$O particles was confirmed by FT-IR spectroscopy, it can be seen that after combined with Cu$_2$O particle, the absorption peak of C-O group vibrations moved to high wavenumber and the intensity become weaker, shown in Fig. S3.

The shape of a face centered cubic (fcc) crystal was mainly determined by the ratio of the growth rate in {100} planes to that in {111} planes. A general order of surface energies associated with the crystallographic planes is γ{111}< γ {100}, so the {111} planes can easily be stabilized.[21] In Cu$_2$O crystal structure, the {100} and {111} surfaces in the Cu$_2$O crystal lattice are different in the surface atom structures. The {100} is a polar surface, but {111} is a nonpolar surface.[22] Murphy *et al* have reported that the preferential adsorption of molecules and ions in solution to different crystal faces makes the nanoparticles develop into various shapes by controlling the growth rates along different crystal axes.[23]
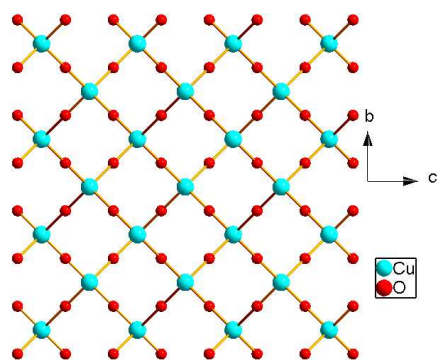
Figure 5. Crystal structures of Cu$_2$O oriented to show the (100) planes.

Carboxylic group plays an important role in inducing the formation of the {100} planes to facilitate the growth of nanocubes and is essential to the shape evolution process. Fig. 5 displays crystal structures of Cu$_2$O oriented to show the {100} planes. Due to the anisotropy in adsorption stability, the additives are adsorbed onto a certain crystallographic plane more strongly than others. This preferential adsorption lowers the surface energy of the bound plane and hinders the crystal growth perpendicular to this plane, resulting in a change in the final morphology. It might be explained in terms of the kinetics of the growth process. The lowest growth direction will determine the final morphology of the crystals [24]. On the basis of the present observations, carboxylic group may be specific for binding to {100} planes. The dominant adsorption of carboxyl group on the {100} planes lower the energy of these facets and drives the growth of nuclei in a 2D mode to produce cubic with confined {100} planes.

The aggregated cubic-like Cu$_2$O microcrystals consisted of a large quantity of Cu$_2$O nanoparticles indicate that the method in our work is a simple and efficient way to prepare Cu$_2$O nano-cubes with exposed {100} planes [25]. Varying the concentration of C-dots during the synthesis led to a dramatic change in the size and shape of these particles. When the Cu$_2$O nuclei are formed in the reaction, the adsorption and desorption of the carboxylic group on {100} planes of the Cu$_2$O nuclei may kinetically dominate the crystal growth direction. When the concentration of copper C-dots solution is 0.05 M (<0.05 M), a faster growth rate of the {111} planes leads to their elimination and the lowest growth direction will determine the final morphology of the crystals. Finally, the preferential crystal growth along <100> directions results in the formation of cubic-shaped crystals Cu$_2$O crystals surrounded by six {100} planes are formed, with diameters from 300 to 400 nm. When the concentration of C-dots solution is increased to 0.1 M (>0.1 M), will cause higher concentration of Cu$_2$O particles and the nucleus grew up quickly, correspondingly higher aggregation centers, which lead to the growth of crystal reached thermodynamics equilibrium before large micro-spheres assembled, in the range 0.7 -2 μm formed. Another important aspect of this synthesis lies in the presence of excess ascorbic acid, which leads to Cu$_2$O can not be quickly oxide into CuO by O$_2$ molecular in the air, and ultimately slow formation of Cu$_2$O nanocrystals. The formation mechanism proposed as is shown in Scheme 1.
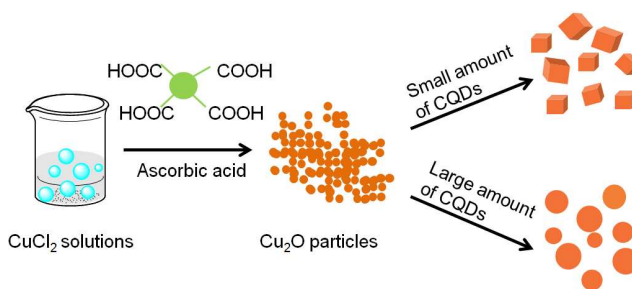
Scheme 1. The possible formation mechanism of the different morphology of Cu$_2$O particles.

On the basis of the above results, it could be concluded that the formation mechanisms of nanocubes and macro-spheres were different. These results clearly confirm that CQDs exhibit much more uniform size/charge characteristics. Nanocubes formed by oriented assembling of tiny nanoparticles under low concentration, mainly determined by the relative growth rate of crystal planes bounding the crystal. When the concentration of carbon dots solution was increased, the nucleus grew up quickly and the growth of crystal reached thermodynamics equilibrium before micro-particles assembled. Thus, the growth of crystals was governed under kinetic control and only nanoparticles formed at high hydrothermal temperatures.

Conclusions

In summary, two different types of nanocrystals of Cu_2O particles have been prepared. We have demonstrated that carbon dots have dramatically effects on the morphology changes of the Cu_2O crystals. The possible formation mechanism has been discussed. This may provide a new and facile way to control the morphology of other semiconductor materials by using carbon dots. These systems will be useful for a broad range of applications such as catalysis, sensors, and optoelectronics where their properties depend on different crysallgraphic planes of the crystals.

Acknowledgements

Notes and references

^{a} Laboratory of Environmental Sciences and Technology, Xinjiang Technical Institute of Physics & Chemistry; Key Laboratory of Functional Materials and Devices for Special Environments, Chinese Academy of Sciences, Urumqi 830011, China. Fax: Fax: +86 0991 383 8957; Tel: +86 0991 383 5879; E-mail: xyfan@ms.xjb.ac.cn; cywang@ms.xjb.ac.cn
^{b} Xinjiang Academy of Safety Science and Technology, 111 Jianguo Road, Urumqi, Xinjiang 830002, China

† Electronic Supplementary Information (ESI) available: [details of any supplementary information available should be included here]. See DOI:10.1039/b000000x/

‡ Footnotes should appear here. These might include comments relevant to but not central to the matter under discussion, limited experimental and spectral data, and crystallographic data.

1   C. M. McShane and K.-S. Choi, *J. Am. Chem. Soc.*, 2009, **131**, 2561.
2   A. Paracchino, V. Laporte, K. Sivula, M. Grätzel and E. Thimsen, *Nat Mater*, 2011, **10**, 456.
3   M. Hara, T. Kondo, M. Komoda, S. Ikeda, J. N. Kondo, K. Domen, K. Shinohara and A. Tanaka, *Chem. Commun.*, 1998, 357.
4   Y. Sun and Y. Xia, *Science*, 2002, **298**, 2176.
5   V. F. Puntes, K. M. Krishnan and A. P. Alivisatos, *Science*, 2001, **291**, 2115.
6   G. Liu, J. C. Yu, G. Q. Lu and H.-M. Cheng, *Chem. Commun.*, 2011, **47**, 6763.
7   Z. Zhong, Y. Fang, W. Lu and C. M. Lieber, *Nano Lett.*, 2005, **5**, 1143.
8   X. Li, H. Gao, C. J. Murphy and L. Gou, *Nano Lett.*, 2004, **4**, 1903.
9   M. Leng, M. Liu, Y. Zhang, Z. Wang, C. Yu, X. Yang, H. Zhang and C. Wang, *J. Am. Chem. Soc.*, 2010, **132**, 17084.
10 C.-H. Kuo and M. H. Huang, *J. Am. Chem. Soc.*, 2008, **130**, 12815.
11 L. Zhang and H. Wang, *ACS nano*, 2011, **5**, 3257.
12 Z. Li and H. C. Zeng, *Chem. Mater.*, 2013, **25**, 1761.
13 W.-C. Huang, L.-M. Lyu, Y.-C. Yang and M. H. Huang, *J. Am. Chem. Soc.*, 2011, **134**, 1261.
14 X. Yang, J. Fu, C. Jin, J. Chen, C. Liang, M. Wu and W. Zhou, *J. Am. Chem. Soc.*, 2010, **132**, 14279.
15 H. Xu and W. Wang, *Angew. Chem. Int. Ed.*, 2007, **46**, 1489.
16 H. Li, R. Liu, R. Zhao, Y. Zheng, W. Chen and Z. Xu, *Cryst. Growth Des.*, 2006, **6**, 2795.
17 X. Wang, L. Cao, S.-T. Yang, F. Lu, M. J. Meziani, L. Tian, K. W. Sun, M. A. Bloodgood and Y.-P. Sun, *Angew. Chem. Int. Ed.*, 2010, **49**, 5310.
18 S. N. Baker and G. A. Baker, *Angew. Chem. Int. Ed.*, 2010, **49**, 6726.
19 H. Liu, T. Ye and C. Mao, *Angew. Chem. Int. Ed.*, 2007, **46**, 6473.
20 A. Ulman, *Chem. Rev.*, 1996, **96**, 1533.
21 H. Y. Zhao,Y. F. Wang and J. H. Zeng, *Cryst. Growth &Des.*, 2008, **8**, 3731.
22 S. M. Lee, S.N. Cho and J. Cheon, *Adv. Mater.* 2003, **15**, 441.
23 C. J. Murphy, *Science,* 2002, **298**, 2139.
24 K. Self, H. Zhou, H. F. Greer, Z. R. Tian and W. Zhou*, Chem. Commun.,* 2013, **49**, 5411.
25 M. J. Siegfried and K.-S. Choi, *J. Am. Chem. Soc.*, 2006, **128**, 10356.